

## Supplementary Information

for

# A Bis(aluminocenophane) with a Short Aluminum–Aluminum Single Bond

<b>Experimental Procedures</b>	<b>1</b>
<b>NMR Spectra</b>	<b>2 – 3</b>
<b>XRD Data</b>	<b>4 – 5</b>
<b>Computational Details</b>	<b>6 – 21</b>
<b>References</b>	<b>22</b>

## Experimental Procedures

All manipulations were carried out under an argon inert gas atmosphere (argon 5.0), using either Schlenk line techniques or a glovebox. Compound **1**<sup>1</sup> and {<sup>Mes</sup>NacNacMg}<sub>2</sub><sup>2</sup> were prepared according to literature known procedures. NMR-spectra were recorded on Bruker Avance III 300 and Bruker Avance III 400 spectrometers. The <sup>1</sup>H and <sup>13</sup>C NMR spectra were referenced using the solvent signals ( $\delta$ <sup>1</sup>H(C<sub>6</sub>D<sub>6</sub>) = 7.16;  $\delta$ <sup>13</sup>C(C<sub>6</sub>D<sub>6</sub>) = 128.06). Elemental analysis were performed on an Elementar vario micro cube. Single crystal X-ray diffraction analysis were carried out at low temperatures on Bruker AXS X8 Apex CCD and Bruker AXS D8 Venture diffractometers operating with graphite monochromated Mo K $\alpha$  radiation. Structure solution and refinement was performed using SHELX<sup>3</sup>.

### Synthesis of bis(aluminocenophane) **2**:

Compound **1** (236 mg / 0.43 mmol) and 1,3- $\beta$ -diketiminate magnesium(I) dimer ({<sup>Mes</sup>NacNacMg}<sub>2</sub>) (307 mg / 0.43 mmol) were charged into a Schlenk flask. 20 mL of toluene were added and the mixture was stirred overnight at room temperature. After filtration, the solution was concentrated and stored at 253 K overnight, resulting in the crystallization of bis(aluminocenophane) **2**. Isolation of the precipitate and drying *in vacuo* yielded the product as a colorless crystalline solid, which can be stored at 248 K under an inert gas atmosphere for at least several weeks.

Yield: 180 mg / 80%

<sup>1</sup>H NMR (400.13 MHz, C<sub>6</sub>D<sub>6</sub>, 298 K):  $\delta$  = 6.08 (t,  $J$  = 2.5 Hz, 8H, Cp-H(C<sub>3</sub>-H)), 5.67 (t,  $J$  = 2.5 Hz, 8H, Cp-H(C<sub>2</sub>-H)), 1.30 (s, 24H, C(CH<sub>3</sub>)<sub>2</sub>).

<sup>13</sup>C{<sup>1</sup>H} NMR (100.62 MHz, C<sub>6</sub>D<sub>6</sub>, 298 K):  $\delta$  = 125.7 (Cp(C1)), 119.7 (Cp(C3)), 106.2 (Cp(C2)), 42.7 (C(CH<sub>3</sub>)<sub>2</sub>), 27.6 (C(CH<sub>3</sub>)<sub>2</sub>).

No signal was observed for a C<sub>6</sub>D<sub>6</sub> solution of **2** in the <sup>27</sup>Al NMR spectrum in the range of +200 to -200 ppm.

Elemental analysis for C<sub>32</sub>H<sub>40</sub>Al<sub>2</sub>: calculated: 80.30% C, 8.42% H; found: 78.18% C, 8.50% H (carbon values were repeatedly reproducibly low even upon analysis of crystalline material, presumably due to the formation of aluminum carbide).

### Reaction of bis(aluminocenophane), **2**, with element chlorides:

Bis(aluminocenophane) **2** (20 mg / 0.04 mmol) and the corresponding element chloride (CCl<sub>4</sub>: 8.2  $\mu$ L / 0.08 mmol; AlCl<sub>3</sub>: 6 mg / 0.04 mmol) were dissolved in 1 mL of deuterated benzene and the solution was stirred for 1 h. Subsequently, insoluble components were filtered off and the mixtures were analyzed by <sup>1</sup>H and <sup>13</sup>C NMR-spectroscopic, which revealed formation of **1**, in case of the reaction with CCl<sub>4</sub> along with some unidentified byproducts.

<sup>1</sup>H NMR (400.13 MHz, C<sub>6</sub>D<sub>6</sub>, 293 K):  $\delta$  = 6.26 (t,  $J$  = 1.9 Hz, 8H, Cp-H), 5.21 (s, 8H, Cp-H), 1.05 (s, 24H, C(CH<sub>3</sub>)<sub>2</sub>).

<sup>13</sup>C{<sup>1</sup>H} NMR (100.62 MHz, C<sub>6</sub>D<sub>6</sub>, 293 K):  $\delta$  = 146.8 (Cp), 128.6 (Cp), 117.6 (Cp), 41.6 (C(CH<sub>3</sub>)<sub>2</sub>), 24.1 (C(CH<sub>3</sub>)<sub>2</sub>).

### Reaction of bis(aluminocenophane), **2**, with *tert*-butyl isocyanide to give **3**:

Bis(aluminocenophane) **2** (20 mg / 0.042 mmol) and *tert*-butyl isocyanide (12 mg / 0.14 mmol) were mixed and dissolved in toluene and the solution was stirred for 16 h at ambient temperature and subsequently cooled down to 248 K overnight, resulting in the precipitation of **3** in form of orange needles. The crystals were separated from the mother liquor and dried *in vacuo*.

Yield: 12 mg / 45%.

<sup>1</sup>H NMR (400.13 MHz, C<sub>6</sub>D<sub>6</sub>, 293 K):  $\delta$  = 6.13-6.11 (m, 4H, Cp-H), 6.07-6.06 (m, 4H, Cp-H), 6.05-6.03 (m, 4H, Cp-H), 5.19 (br s, 4H, Cp-H), 1.48 (s, 12H, C(CH<sub>3</sub>)<sub>2</sub>), 1.45 (s, 12H, C(CH<sub>3</sub>)<sub>2</sub>), 1.18 (s, 18H, CNC(CH<sub>3</sub>)<sub>3</sub>).

<sup>13</sup>C{<sup>1</sup>H} NMR (75.48 MHz, C<sub>6</sub>D<sub>6</sub>, 296 K):  $\delta$  = 146.6 (Cp), 128.6 (Cp), 120.4 (Cp), 116.1 (Cp), 109.6 (Cp), 86.8 (br, CNC(CH<sub>3</sub>)<sub>3</sub>), 59.0 (CNC(CH<sub>3</sub>)<sub>3</sub>), 42.6 (C(CH<sub>3</sub>)<sub>2</sub>), 29.7 (CNC(CH<sub>3</sub>)<sub>3</sub>), 27.1 (C(CH<sub>3</sub>)<sub>2</sub>), 26.1 (C(CH<sub>3</sub>)<sub>2</sub>).

No signal was observed in the <sup>27</sup>Al NMR spectrum of a C<sub>6</sub>D<sub>6</sub> solution in the range of +200 to -200 ppm.

Elemental analysis for C<sub>42</sub>H<sub>58</sub>Al<sub>2</sub>N<sub>2</sub>: calculated: 78.22% C, 9.07% H, 4.34% N; found: 77.22% C, 9.24% H, 4.19% N (carbon value was repeatedly reproducibly low even upon analysis of crystalline material, presumably due to the formation of aluminum carbide).

## NMR Spectra

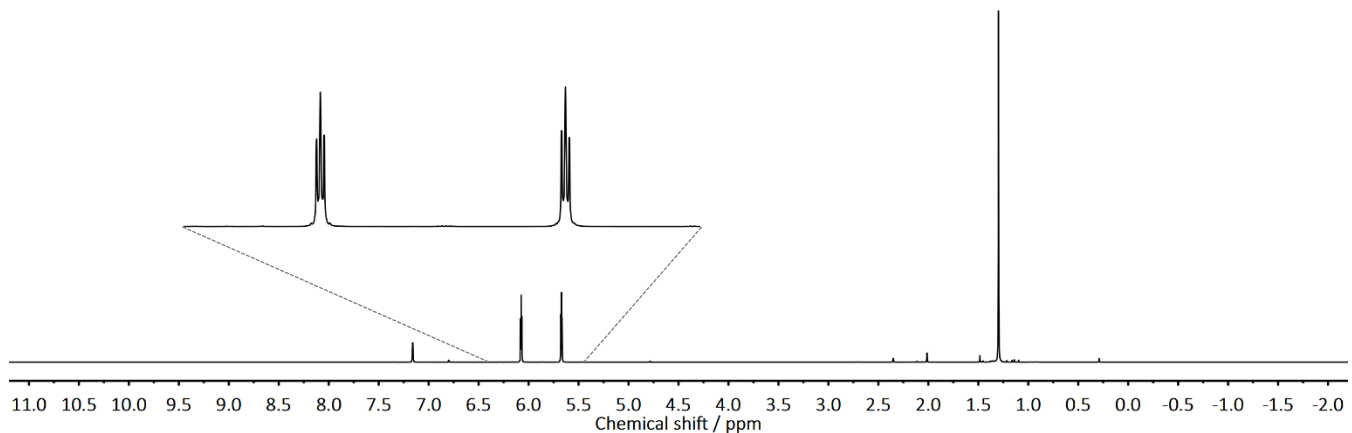


Figure S1. <sup>1</sup>H NMR spectrum of **2** (400.13 MHz, C<sub>6</sub>D<sub>6</sub>, 298 K).

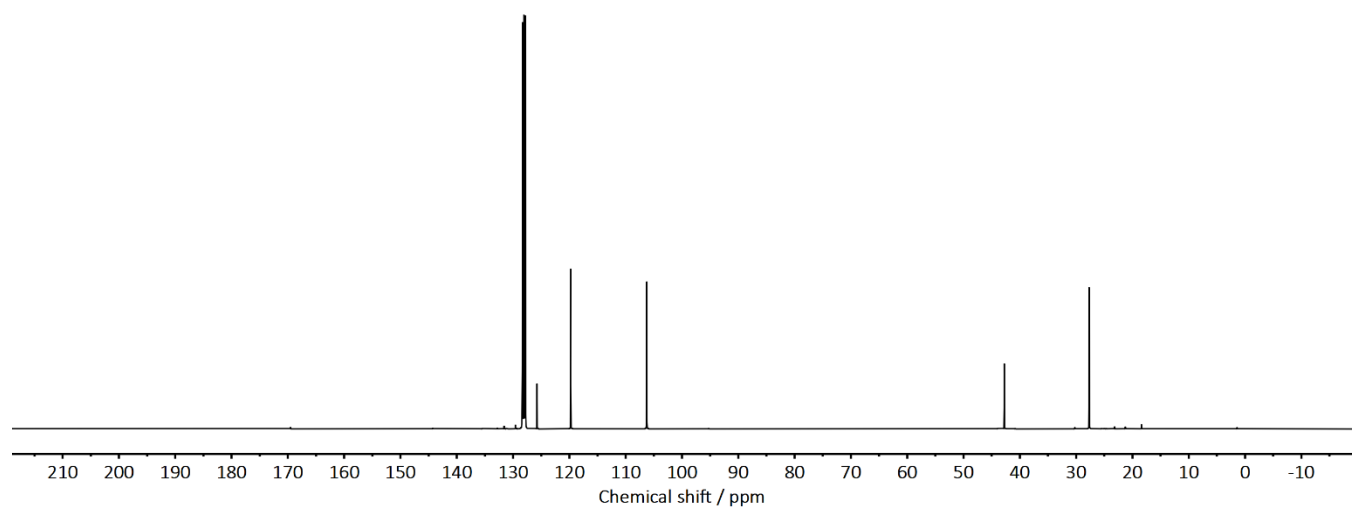
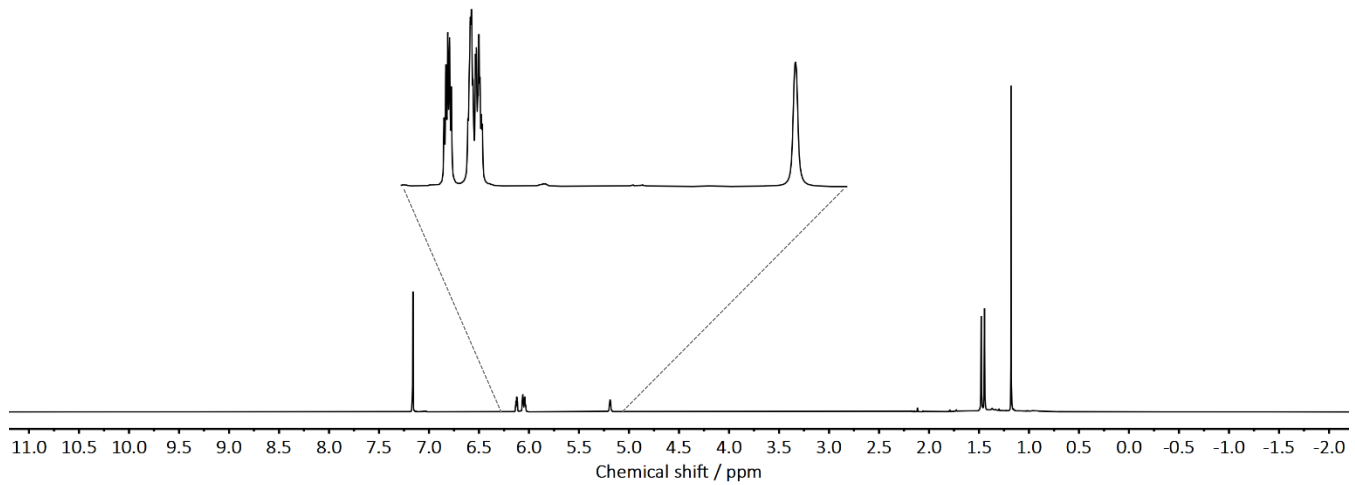
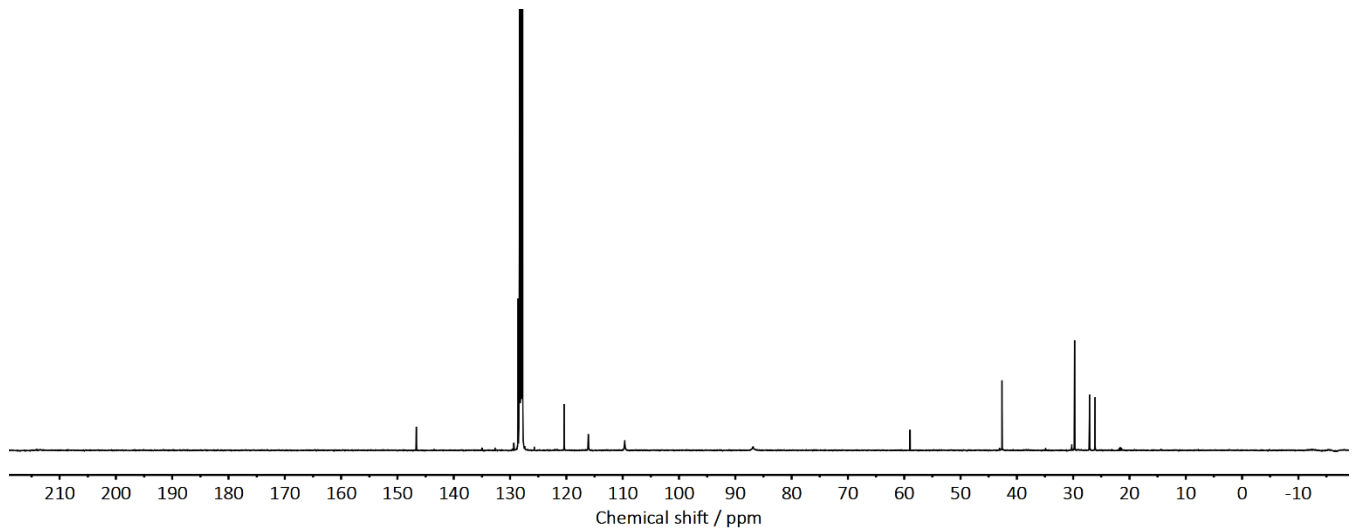


Figure S2. <sup>13</sup>C{<sup>1</sup>H} NMR spectrum of **2** (100.62 MHz, C<sub>6</sub>D<sub>6</sub>, 298 K).



**Figure S3.**  $^1\text{H}$  NMR spectrum of **3** (400.13 MHz,  $\text{C}_6\text{D}_6$ , 294 K).



**Figure S4.**  $^{13}\text{C}\{\text{H}\}$  NMR spectrum of **3** (100.62 MHz,  $\text{C}_6\text{D}_6$ , 293 K).

---

## XRD data

Crystal structure data has been deposited with the Cambridge Crystallographic Data Centre (CCDC) and is available free of charge from the Cambridge Structural Database (see reference numbers).

### Crystallographic data for 2

CCDC reference number:	1936579
Empirical formula	C <sub>32</sub> H <sub>40</sub> Al <sub>2</sub>
Formula weight	478.60
Temperature	122(2) K
Wavelength	0.71073 Å
Crystal system	orthorhombic
Space group	P2 <sub>1</sub> 2 <sub>1</sub> 2 <sub>1</sub>
Unit cell dimensions	a = 8.9879(3) Å $\alpha$ = 90° b = 10.9776(3) Å $\beta$ = 90° c = 26.2559(7) Å $\gamma$ = 90°
Volume	2590.55(13) Å <sup>3</sup>
Z	4
Density (calculated)	1.227 Mg/m <sup>3</sup>
Absorption coefficient	0.131 mm <sup>-1</sup>
F(000)	1032
Crystal size	0.438 x 0.322 x 0.228 mm <sup>3</sup>
Theta range for data collection	1.551 to 32.766°
Index ranges	-13<=h<=13, -16<=k<=16, -39<=l<=39
Reflections collected	46884
Independent reflections	9536 [R(int) = 0.0232]
Completeness to theta = 25.242°	100.0%
Absorption correction	semi-empirical from equivalents
Max. and min. transmission	0.7464 and 0.7238
Refinement method	full-matrix least-squares on F <sup>2</sup>
Data / restraints / parameters	9536 / 0 / 467
Goodness-of-fit on F <sup>2</sup>	1.052
Final R indices [I>2sigma(I)]	R1 = 0.0286, wR2 = 0.0717
R indices (all data)	R1 = 0.0316, wR2 = 0.0733
Absolute structure parameter	0.02(2)
Extinction coefficient	n/a
Largest diff. peak and hole	0.301 and -0.200 e.Å <sup>-3</sup>

---

### Crystallographic data for 3

CCDC reference number:	1936580
Empirical formula	C <sub>42</sub> H <sub>58</sub> Al <sub>2</sub> N <sub>2</sub>
Formula weight	644.86
Temperature	133(2) K
Wavelength	0.71073 Å
Crystal system	triclinic
Space group	P-1
Unit cell dimensions	a = 11.2373(4) Å b = 13.3899(4) Å c = 14.1649(5) Å
	α = 63.7160(13)° β = 70.0821(13)° γ = 80.4239(13)°
Volume	1796.37(11) Å <sup>3</sup>
Z	2
Density (calculated)	1.192 Mg/m <sup>3</sup>
Absorption coefficient	0.113 mm <sup>-1</sup>
F(000)	700
Crystal size	0.535 x 0.179 x 0.110 mm <sup>3</sup>
Theta range for data collection	2.844 to 47.880°
Index ranges	-23<=h<=23, -27<=k<=27, -29<=l<=29
Reflections collected	227033
Independent reflections	34041 [R(int) = 0.0545]
Completeness to theta = 25.242°	99.1%
Absorption correction	semi-empirical from equivalents
Max. and min. transmission	0.7494 and 0.6929
Refinement method	full-matrix least-squares on F <sup>2</sup>
Data / restraints / parameters	34041 / 167 / 546
Goodness-of-fit on F <sup>2</sup>	1.036
Final R indices [I>2sigma(I)]	R1 = 0.0435, wR2 = 0.1142
R indices (all data)	R1 = 0.0752, wR2 = 0.1357
Extinction coefficient	n/a
Largest diff. peak and hole	0.552 and -0.468 e.Å <sup>-3</sup>

## Computational Details

All geometries were optimized without symmetry constraint within the DFT (density functional theory) framework using the M06-2X<sup>4</sup> in combination with the Ahlrichs def2-TZVPP basis function. In addition, we optimized compounds **2**, Al<sub>2</sub>H<sub>4</sub> and Al<sub>2</sub>Cl<sub>4</sub> using BP86+D3(BJ)/def2-TZVPP,<sup>5</sup> for comparison. These calculations were performed using the Gaussian 16 B.01 software.<sup>6</sup> The stationary points were located with the Berny algorithm<sup>7</sup> using redundant internal coordinates. Analytical Hessians were computed to determine the nature of stationary points (one and zero imaginary frequencies for transition states and minima, respectively)<sup>8</sup> and to calculate unscaled zero-point energies (ZPEs) as well as thermal corrections and entropy effects using the standard statistical-mechanics relationships for an ideal gas. We performed single point calculations on the M06-2X-optimized structures with local couple cluster (LCCSD(T)) method<sup>9</sup> by employing MOLPRO 2019.1<sup>10</sup> software program package. Density fitting (DF) approximation have been used in the local method.<sup>11</sup> The cc-pVTZ basis set was used for carbon, hydrogen, aluminum and chloride. In the density fitting calculation we used cc-pVTZ/JKFIT auxiliary fitting basis sets<sup>12</sup> in DF-HF calculations. The Wiberg Bond Indices (WBI)<sup>13</sup> and NPA<sup>14</sup> atomic partial charges have been calculated at the M06-2X/def2-TZVPP level of theory using GENNBO 6.0 programs.<sup>15</sup> The Atoms-in-Molecule (AIM) method<sup>16</sup> was performed at the M06-2X/def2-TZVPP level of theory with the program AIMAll program package.<sup>17</sup> The nature of the chemical bond was investigated by means of an energy decomposition analysis (EDA), which was developed by Morokuma<sup>18</sup> and by Ziegler and Rauk.<sup>19</sup> The EDA focuses on the instantaneous interaction energy  $\Delta E_{int}$  of a bond A-B between the fragments A and B in the particular electronic reference state at the frozen geometry of the molecule AB.<sup>20</sup> The interaction energy  $\Delta E_{int}$  is divided into four main components [Eq. (1)].

$$\Delta E_{int} = \Delta E_{elstat} + \Delta E_{Pauli} + \Delta E_{orb} + \Delta E_{disp} \quad (1)$$

The term  $\Delta E_{elstat}$  corresponds to the quasiclassical electrostatic interaction between the unperturbed charge distributions of the prepared atoms and is usually attractive. The Pauli repulsion  $\Delta E_{Pauli}$  arises as the energy change associated with the transformation from the superposition of the unperturbed electron densities  $\rho^A + \rho^B$  of the isolated fragments to the wavefunction  $\Psi^0 = \hat{N}[\Psi_A \Psi_B]$ , which properly obeys the Pauli principle through explicit antisymmetrization ( $\hat{A}$  operator) and renormalization ( $N = \text{constant}$ ) of the product wavefunction.  $\Delta E_{Pauli}$  comprises the destabilizing interactions between electrons of the same spin on either fragment. The orbital interaction  $\Delta E_{orb}$  accounts for charge transfer, polarization effects and electron-pair bonding.<sup>21</sup> In the case that the Grimme dispersion corrections<sup>22</sup> are computed the term  $\Delta E_{disp}$  is added to the equation to count the dispersion interaction between the fragments (BP86+D3(BJ) method), while when a meta hybrid functional (M06-2X) is used the meta hybrid correction is counted ( $\Delta E_{metahybrid}$ ). The relaxation of the fragments to their equilibrium geometries at the electronic ground state is termed  $\Delta E_{prep}$ , because it may be considered as preparation energy for chemical bonding. The addition of  $\Delta E_{prep}$  to the intrinsic interaction energy  $\Delta E_{int}$  gives the total energy  $\Delta E$ , which is - by definition with opposite sign - the bond dissociation energy  $D_e$ :

$$\Delta E (-D_e) = \Delta E_{int} + \Delta E_{prep} \quad (2)$$

The EDA–NOCV method combines the EDA with the natural orbitals for chemical valence (NOCV) to decompose the orbital interaction term  $\Delta E_{orb}$  into pairwise contributions. The NOCVs  $\Psi_i$  are defined as the eigenvector of the valence operator,  $\hat{V}$ , given by Equation (3).

$$\hat{V}\Psi_i = v_i \Psi_i \quad (3)$$

In the EDA–NOCV scheme the orbital interaction term,  $\Delta E_{orb}$ , is given by Equation (4),

$$\Delta E_{orb} = \sum_k \Delta E_k^{orb} = \sum_{k=1}^N v_k [-F_{-k,-k}^{TS} + F_{k,k}^{TS}] \quad (4)$$

in which  $F_{-k,-k}^{TS}$  and  $F_{k,k}^{TS}$  are diagonal transition state Kohn–Sham matrix elements corresponding to NOCVs with the eigenvalues  $-v_k$  and  $v_k$ , respectively. The  $\Delta E_k^{orb}$  term for a particular type of bond is assigned by visual inspection of the shape of the deformation density  $\Delta \rho_k$ . The latter term is a measure of the size of the charge deformation and it provides a visual notion of the charge flow that is associated with the pairwise orbital interaction. The EDA–NOCV scheme thus provides both qualitative and quantitative information about the strength of orbital interactions in chemical bonds. The EDA–NOCV calculations were carried out with program package ADF2018.105<sup>23</sup> using DFT functional BP86<sup>5a,24</sup> with Grimme dispersion corrections D3(BJ)<sup>22</sup> and M06-2X with uncontracted Slater-type orbitals (STOs)<sup>25</sup> with TZ2P quality as basis functions. The latter basis sets for all elements have triple- $\zeta$  quality augmented by two sets of polarization functions. An auxiliary set of s, p, d, f, and g STOs was used to fit the molecular densities and to represent the Coulomb and exchange potentials accurately in each SCF cycle.<sup>26</sup> Scalar relativistic effects have been incorporated by applying the zeroth-order regular approximation (ZORA).<sup>27</sup> The EDA-NOCV calculations at BP86+D3(BJ)/TZ2P and M06-2X/TZ2P level were performed using M06-2X/def2-TZVPPP optimized geometries.

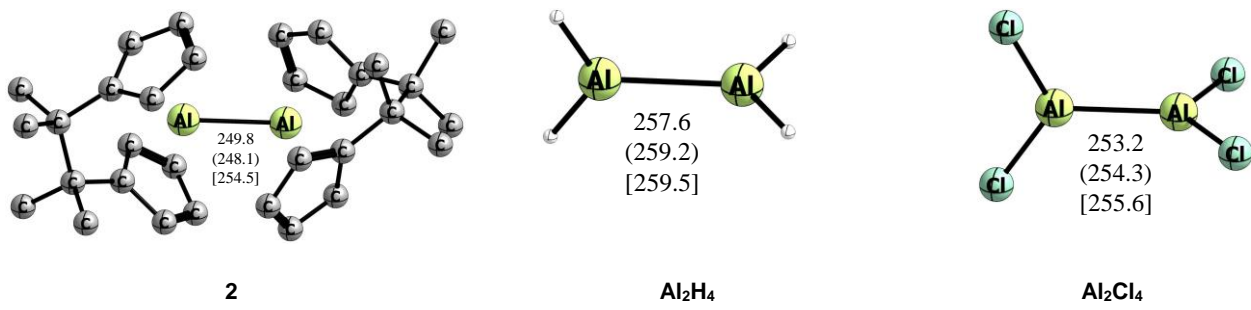


**Figure S5.** Optimized structures of **2**, Al<sub>2</sub>H<sub>4</sub> and Al<sub>2</sub>Cl<sub>4</sub> at the M06-2X/def2-TZVPP (BP86+D3(BJ)/def2-TZVPP) [BP86/def2-TZVPP] level of theory (bond lengths in pm, hydrogen atoms of **2** omitted).

**Table S1.** NBO results at the M06-2X/def2-TZVPP level of theory of compounds **2**, Al<sub>2</sub>H<sub>4</sub> and Al<sub>2</sub>Cl<sub>4</sub>: Wiberg bond order (P) and partial charges (q).

	<b>2</b>	<b>Al<sub>2</sub>H<sub>4</sub></b>	<b>Al<sub>2</sub>Cl<sub>4</sub></b>
q(Al)	+1.25	+0.76	+1.05
P(Al-Al)	0.93	0.90	0.89

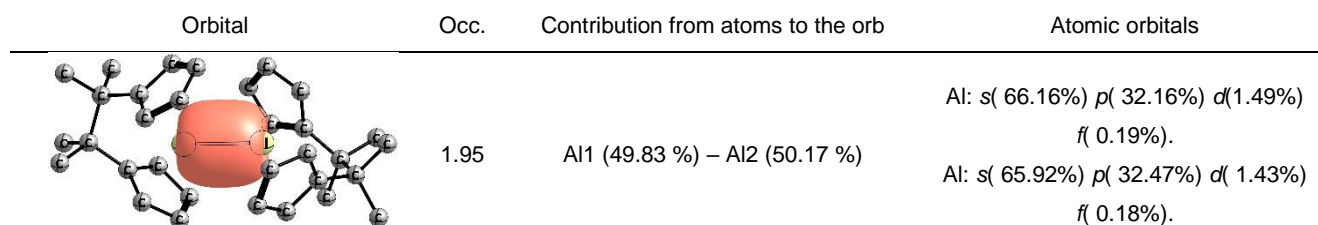


**Figure S6.** NBO results at the M06-2X/def2-TZVPP of **2**. Hydrogen atoms were omitted for clarity.

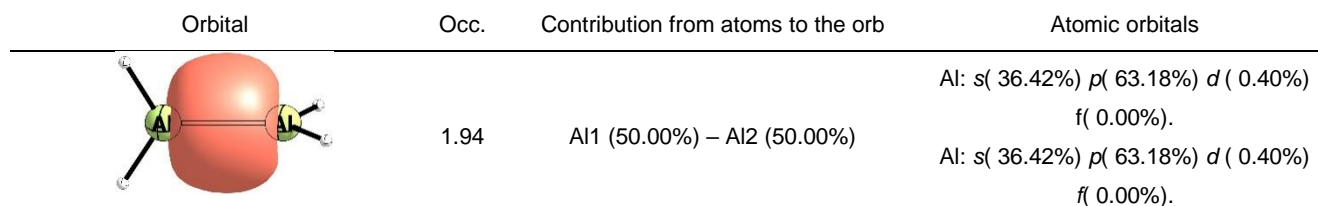


**Figure S7.** NBO results at the M06-2X/def2-TZVPP of  $\text{Al}_2\text{H}_4$ .

Orbital	Occ.	Contribution from atoms to the orb	Atomic orbitals
	1.95	Al1 (50.00%) – Al2 (50.00%)	Al: s( 46.34%) p( 52.94%) d( 0.71%) f( 0.00%). Al: s( 46.34%) p( 52.94%) d( 0.71%) f( 0.00%).

Figure S8. NBO results at the M06-2X/def2-TZVPP of  $\text{Al}_2\text{Cl}_4$ .

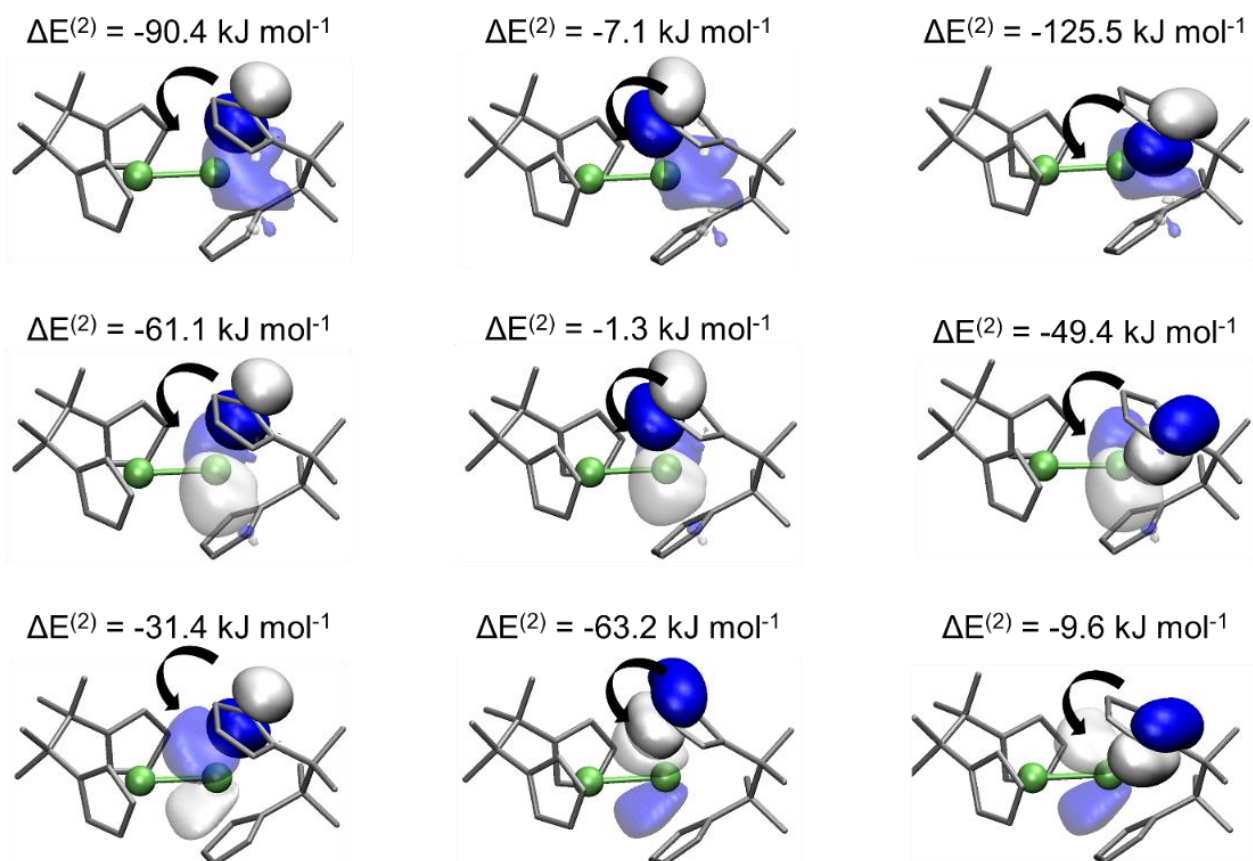
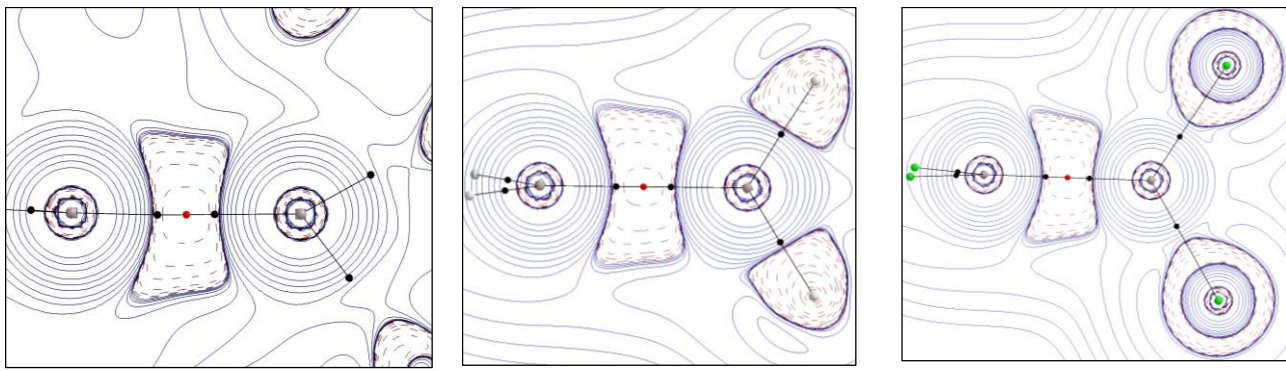


Figure S9. Second Order Perturbation interaction within the NBO analysis at the M06-2X/def2-TZVPP of **2**.



**2**

**Al<sub>2</sub>H<sub>4</sub>**

**Al<sub>2</sub>Cl<sub>4</sub>**

**Figure S10.** Laplacian distribution  $\nabla^2\rho(r)$  in the Al-Al-X ( $X = \text{Cp}^{\text{centroid}}$ , H, Cl) plane of **2**, Al<sub>2</sub>H<sub>4</sub> and Al<sub>2</sub>Cl<sub>4</sub>. Dashed red lines indicate areas of charge concentration ( $\nabla^2\rho(r) < 0$ ), while solid blue lines show areas of charge depletion ( $\nabla^2\rho(r) > 0$ ). The solid black lines connecting the atomic nuclei are the bond paths, the small black dots are the bond critical points (BCP) and the small red dots are the Non-Nuclear Attractors (NNA).

**Table S2.** Calculated electron densities  $\rho$  (in e/bohr<sup>3</sup>) at the Bond Critical Points (BCP) and Non-Nuclear Attractors (NNA) at the M06-2X/def2-TZVPP level of theory.

	$\rho(\text{BCP1})$	$\rho(\text{BCP2})$	$\rho(\text{NNA})$
<b>2</b>	0.063	0.063	0.064
Al <sub>2</sub> H <sub>4</sub>	0.058	0.058	0.060
Al <sub>2</sub> Cl <sub>4</sub>	0.062	0.062	0.064

**Table S3.** Energy decomposition analysis (EDA) of Al-Al bond for **2**, Al<sub>2</sub>H<sub>4</sub> and Al<sub>2</sub>Cl<sub>4</sub> at BP86+D3(BJ)/TZ2P//M06-2X/def2-TZVPP (energies are in kJ mol<sup>-1</sup>).<sup>a</sup>

	<b>2</b>	Al <sub>2</sub> H <sub>4</sub>	Al <sub>2</sub> Cl <sub>4</sub>
$\Delta E_{\text{int}}$	-315.9	-256.9	-262.0
$\Delta E_{\text{Pauli}}$	406.1	295.3	248.0
$\Delta E_{\text{disp}}^{\text{a}}$	-90.0 (12.5 %)	-6.5 (1.2 %)	-13.5 (2.6 %)
$\Delta E_{\text{elstat}}^{\text{a}}$	-336.7 (46.6 %)	-293.4 (53.1 %)	-228.4 (44.8 %)
$\Delta E_{\text{orb}}^{\text{a}}$	-295.4 (46.9 %)	-252.3 (45.7 %)	-268.2 (52.6 %)
$\Delta E_{\text{prep}}$	22.6	7.4	9.8
$-D_e = \Delta E$	-293.3	-249.5	-252.3

<sup>a</sup>The value in parentheses gives the percentage contribution to the total attractive interactions  $\Delta E_{\text{elstat}} + \Delta E_{\text{orb}} + \Delta E_{\text{disp}}$ .

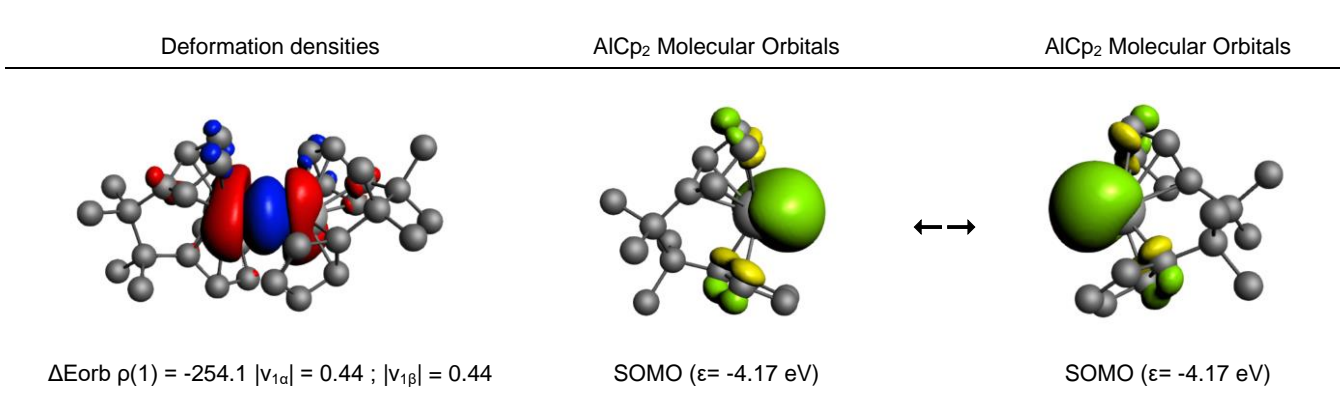


**Figure S11.** Deformation densities  $\Delta p$  (isovalue 0.001 a.u.) at M06-2X/TZ2P//M06-2X/def2-TZVPP of the pairwise orbital interactions between AlCp<sub>2</sub> fragments within compound **2**. For the deformation densities the red color shows the charge outflow, whereas blue shows charge density accumulation.

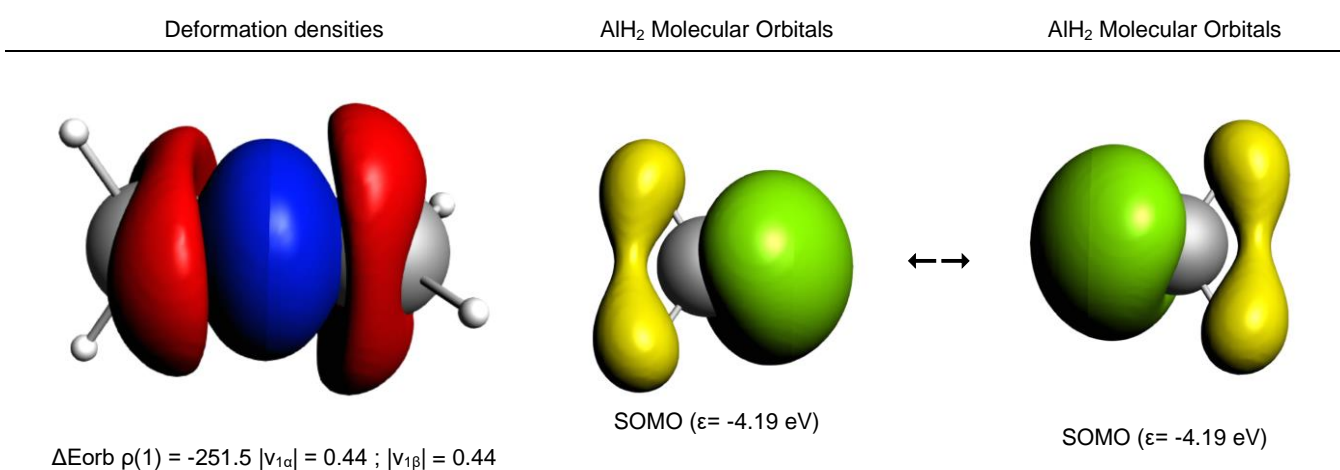


**Figure S12.** Deformation densities  $\Delta p$  (isovalue 0.001 a.u.) at M06-2X/TZ2P//M06-2X/def2-TZVPP of the pairwise orbital interactions between AlH<sub>2</sub> fragments within compound Al<sub>2</sub>H<sub>4</sub>. For the deformation densities the red color shows the charge outflow, whereas blue shows charge density accumulation.

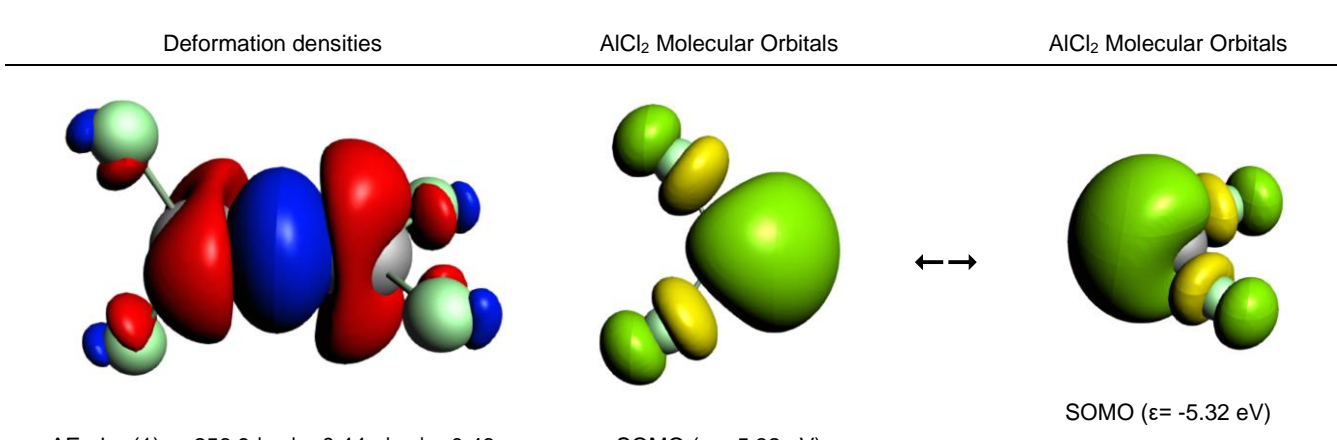


**Figure S13.** Deformation densities  $\Delta\rho$  (isovalue 0.001 a.u.) at M06-2X/TZ2P//M06-2X/def2-TZVPP of the pairwise orbital interactions between AlCl<sub>2</sub> fragments within compound Al<sub>2</sub>Cl<sub>4</sub>. For the deformation densities the red color shows the charge outflow, whereas blue shows charge density accumulation.

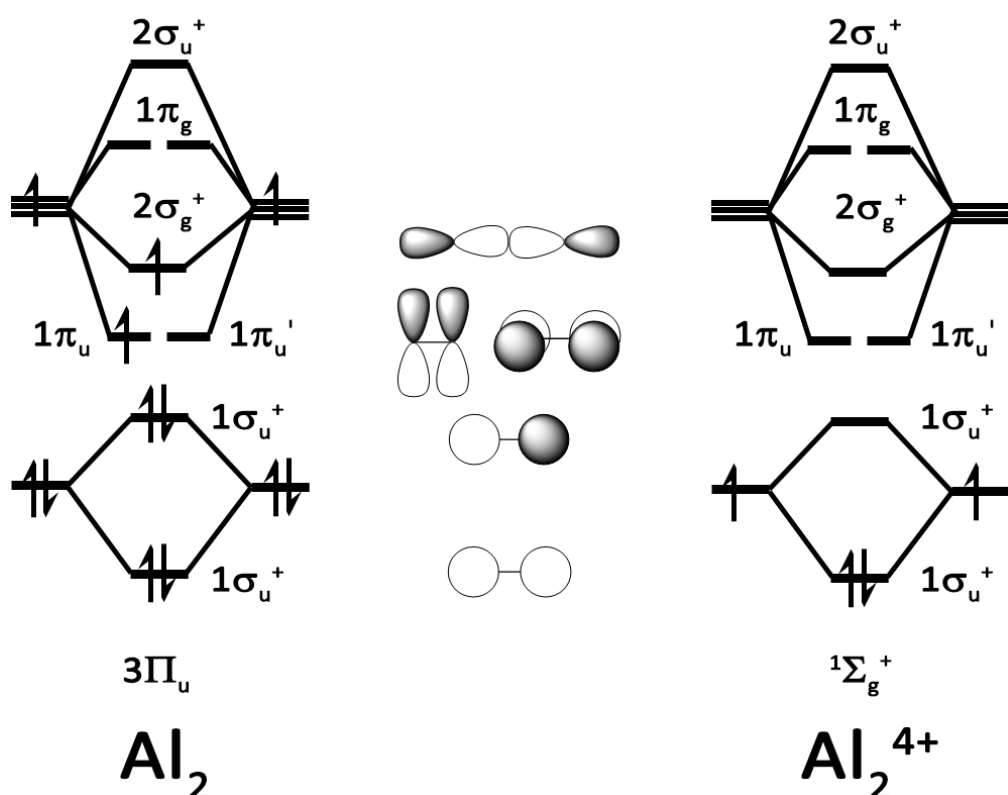


**Figure S14.** Schematic view of relevant electronic states of Al<sub>2</sub> and Al<sub>2</sub><sup>4+</sup>.

**Table S4.** Energy decomposition analysis (EDA) of **2** at BP86+D3(BJ)/TZ2P//M06-2X/def2-TZVPP (energies are in kJ mol<sup>-1</sup>).

	$\text{Al}_2^{4+}(\text{n } \sigma_g^+)^2 (\text{n } \sigma_u^+)^0 ((\text{n}+1) \sigma_g^+)^0 (\pi_u)^0$ $(\pi' u)^0, (\text{Cp}_2(\text{CM}\text{e}_2))_2^{4-}$	$\text{Al}_2(\text{n } \sigma_g^+)^2 (\text{n } \sigma_u^+)^1 ((\text{n}+1) \sigma_g^+)^1 (\pi_u)^1$ $(\pi' u)^1, (\text{Cp}_2(\text{CM}\text{e}_2))_2$
$\Delta E_{int}$	-8538.1	-1254.6
$\Delta E_{Pauli}$	732.5	4056.6
$\Delta E_{disp}^a$	-78.0 (0.8 %)	-78.0 (1.5 %)
$\Delta E_{elstat}^a$	-5881.6 (63.4 %)	-2180.8 (41.1 %)
$\Delta E_{orb}^a$	-3310.9 (35.7 %)	-3052.4 (57.5 %)
$\Delta E_{orb \rho 1}^b$	-477.4 (14.4 %)	
$\Delta E_{orb \rho 2}^b$	-379.8 (11.5 %)	
$\Delta E_{orb \rho 3}^b$	-290.7 (8.8 %)	
$\Delta E_{orb \rho 4}^b$	-277.7 (8.4 %)	
$\Delta E_{orb \rho 5}^b$	-193.4 (5.8 %)	
$\Delta E_{orb \rho 6}^b$	-193.8 (5.9 %)	
$\Delta E_{orb \rho 7}^b$	-198.1 (6.0 %)	

[a] The value in parentheses gives the percentage contribution to the total attractive interactions  $\Delta E_{elstat} + \Delta E_{orb} + \Delta E_{disp}$

**Table S5.** Energy decomposition analysis (EDA) of  $\text{Al}_2\text{H}_4$  at BP86+D3(BJ)/TZ2P//M06-2X/def2-TZVPP (energies are in kJ mol<sup>-1</sup>).

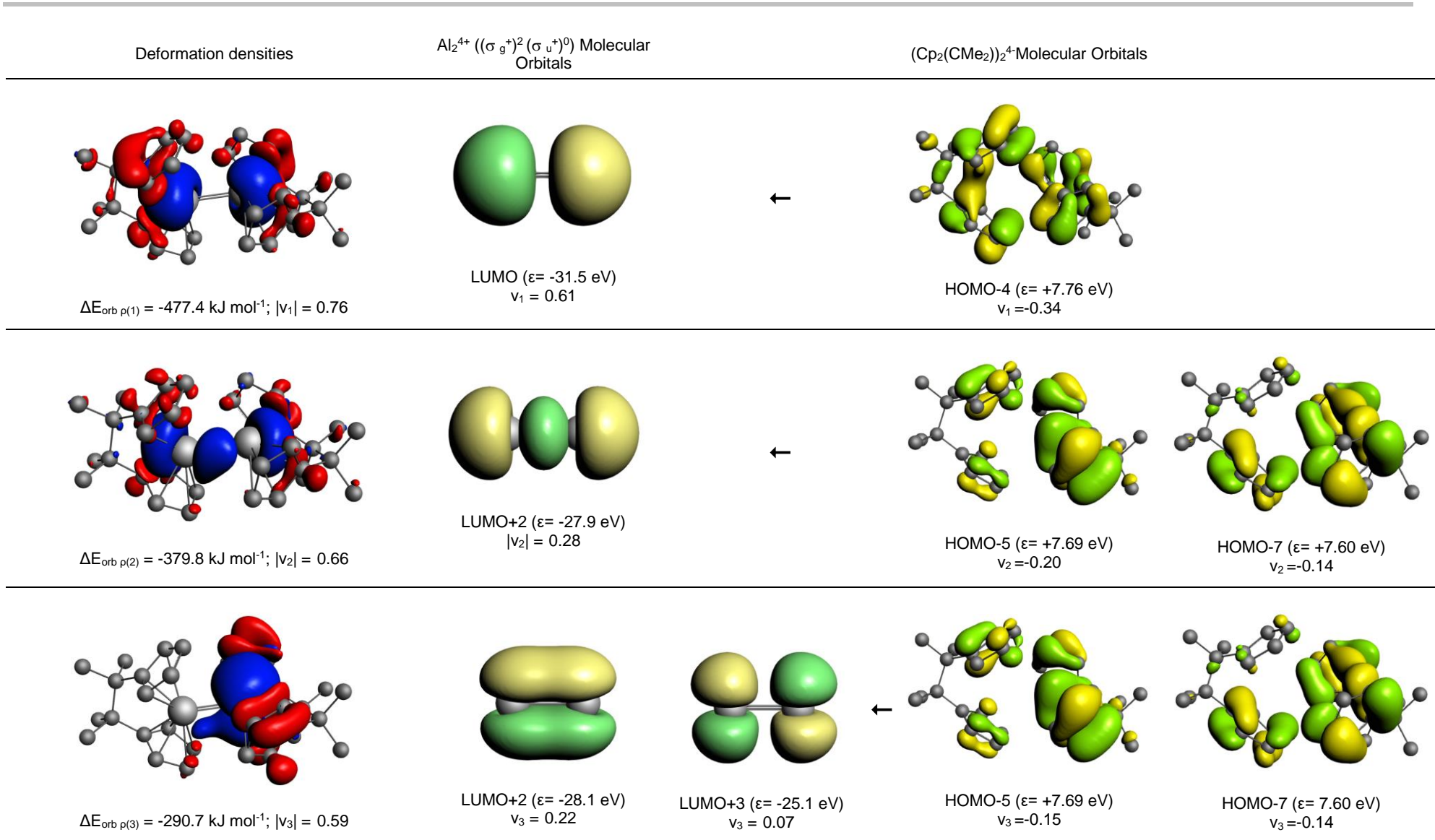
	$\text{Al}_2^{4+}(\text{n } \sigma_g^+)^2 (\text{n } \sigma_u^+)^0 ((\text{n}+1) \sigma_g^+)^0 (\pi_u)^0$ $(\pi' u)^0, (\text{H})_4^{4-}$	$\text{Al}_2(\text{n } \sigma_g^+)^2 (\text{n } \sigma_u^+)^1 ((\text{n}+1) \sigma_g^+)^1 (\pi_u)^1 (\pi' u)^1$ $(\text{H})_4$
$\Delta E_{int}$	-9510.5	-1355.1
$\Delta E_{Pauli}$	1383.5	439.1
$\Delta E_{disp}^a$	1.0 (0.0 %)	1.0 (0.0 %)
$\Delta E_{elstat}^a$	-8344.2 (76.6 %)	-460.5 (25.7 %)
$\Delta E_{orb}^a$	-2550.7 (23.4 %)	-1334.7 (74.4 %)

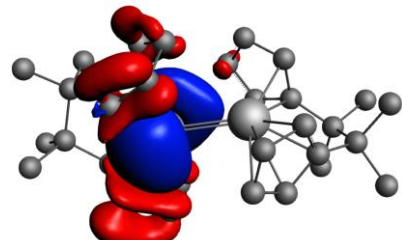
[a] The value in parentheses gives the percentage contribution to the total attractive interactions  $\Delta E_{elstat} + \Delta E_{orb} + \Delta E_{disp}$

**Table S6.** Energy decomposition analysis (EDA) of **2** at M06-2X/TZ2P//M06-2X/def2-TZVPP (energies are in kJ mol<sup>-1</sup>).

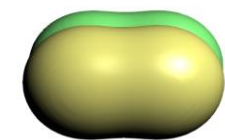
Al <sub>2</sub> <sup>4+</sup> (σ <sub>g</sub> <sup>+</sup> ) <sup>2</sup> (σ <sub>u</sub> <sup>+</sup> ) <sup>0</sup> , (Cp <sub>2</sub> (CMe <sub>2</sub> ) <sub>2</sub> ) <sup>4-</sup>	
ΔE <sub>int</sub>	-8570.4
ΔE <sub>Pauli</sub>	671.4
ΔE <sub>elstat<sup>a</sup></sub>	-6149.2 (66.2 %)
ΔE <sub>orb<sup>a</sup></sub>	-3137.4 (33.8 %)
ΔE <sub>MetaHybrid<sup>a</sup></sub>	44.7
ΔE <sub>orb ρ<sub>1</sub><sup>b</sup></sub>	-430.9 (13.7 %)
ΔE <sub>orb ρ<sub>2</sub><sup>b</sup></sub>	-333.8 (10.6 %)
ΔE <sub>orb ρ<sub>3</sub><sup>b</sup></sub>	-266.3 (8.5 %)
ΔE <sub>orb ρ<sub>4</sub><sup>b</sup></sub>	-262.0 (8.4 %)
ΔE <sub>orb ρ<sub>5</sub><sup>b</sup></sub>	-206.1 (6.6 %)
ΔE <sub>orb ρ<sub>6</sub><sup>b</sup></sub>	-204.0 (6.5 %)
ΔE <sub>orb ρ<sub>7</sub><sup>b</sup></sub>	-152.6 (4.9 %)

[a] The value in parentheses gives the percentage contribution to the total attractive interactions ΔE<sub>elstat</sub> + ΔE<sub>orb</sub> + ΔE<sub>disp</sub>



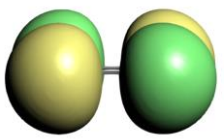


$$\Delta E_{\text{orb } p(4)} = -277.7 \text{ kJ mol}^{-1}; |v_4| = 0.56,$$



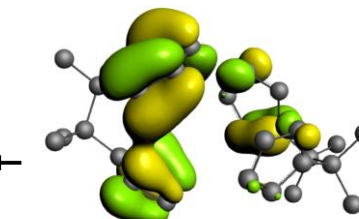
LUMO+2 ( $\epsilon = -28.1 \text{ eV}$ )

$$v_4 = 0.18$$



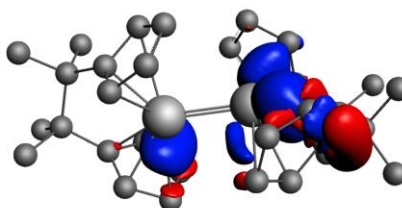
LUMO+3 ( $\epsilon = -25.1 \text{ eV}$ )

$$v_4 = 0.10$$

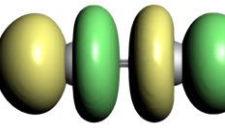


HOMO-6 ( $\epsilon = +7.66 \text{ eV}$ )

$$v_4 = -0.26$$

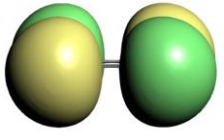


$$\Delta E_{\text{orb } p(5)} = -193.4 \text{ kJ mol}^{-1}; |v_5| = 0.41$$



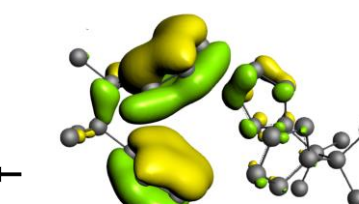
LUMO+4 ( $\epsilon = -25.1 \text{ eV}$ )

$$v_5 = 0.03$$



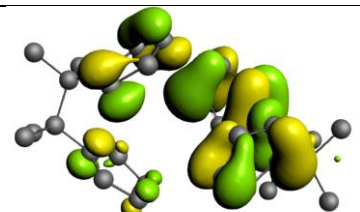
LUMO+3 ( $\epsilon = -25.1 \text{ eV}$ )

$$v_5 = 0.03$$



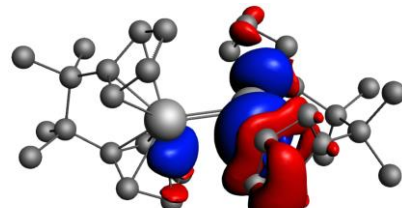
HOMO-9 ( $\epsilon = +4.41 \text{ eV}$ )

$$v_5 = -0.06$$

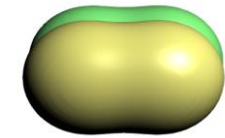


HOMO-1 ( $\epsilon = +8.30 \text{ eV}$ )

$$v_5 = -0.05$$

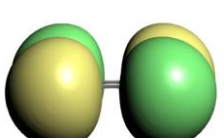


$$\Delta E_{\text{orb } p(6)} = -193.8 \text{ kJ mol}^{-1}; |v_6| = 0.39$$



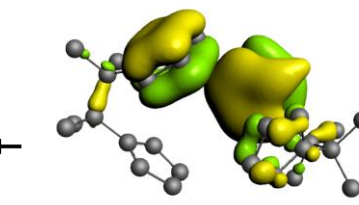
LUMO+2 ( $\epsilon = -28.1 \text{ eV}$ )

$$v_6 = 0.08$$



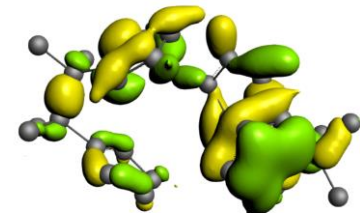
LUMO+3 ( $\epsilon = -25.1 \text{ eV}$ )

$$v_6 = 0.10$$



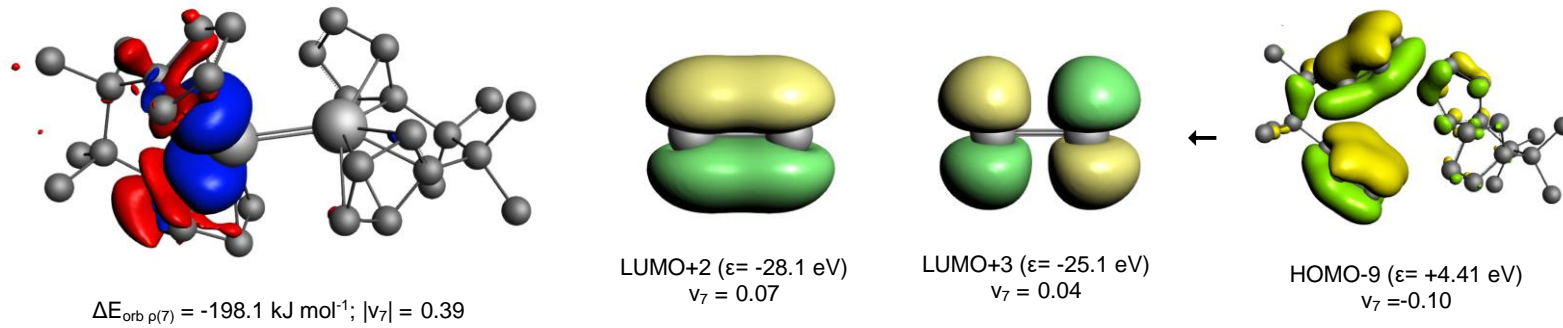
HOMO-8 ( $\epsilon = +4.46 \text{ eV}$ )

$$v_6 = -0.04$$

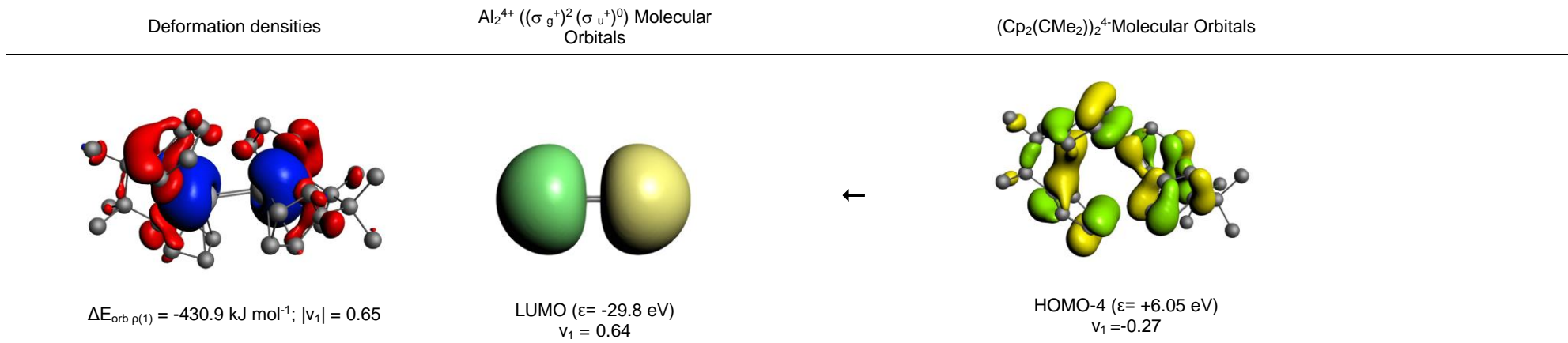


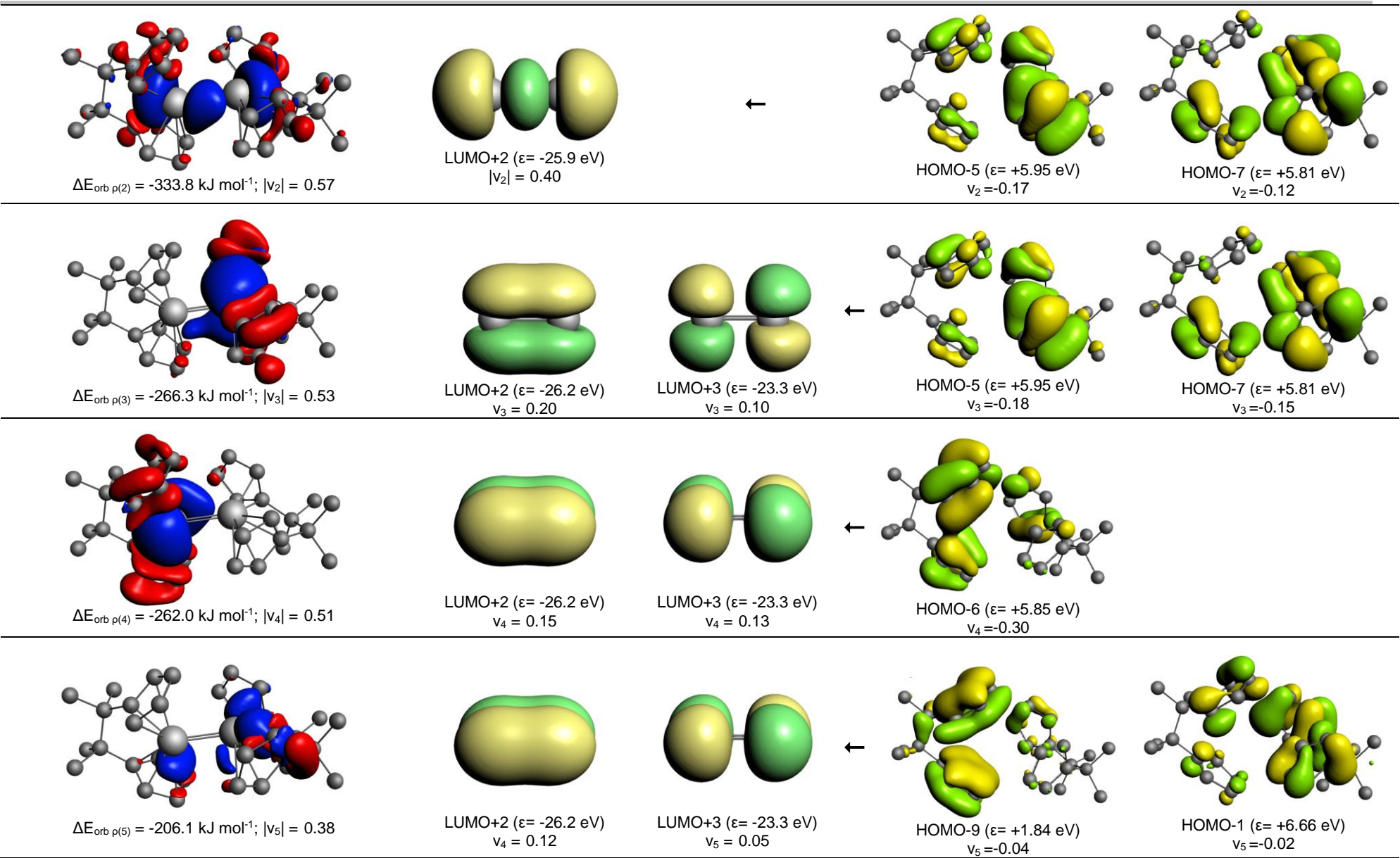
HOMO-10 ( $\epsilon = +4.37 \text{ eV}$ )

$$v_6 = -0.07$$



**Figure S15.** Deformation densities  $\Delta p$  (isovalue 0.001 a.u.) at BP86+D3(BJ)/TZ2P//M06-2X/def2-TZVPP of the pairwise orbital interactions between  $\text{Al}_2^{4+} ((\sigma_g^+)^2 (\sigma_u^+)^0)$  with  $(\text{Cp}_2(\text{CMe}_2))_2^{4-}$  within compound **2**. For the deformation densities the red color shows the charge outflow, whereas blue shows charge density accumulation.





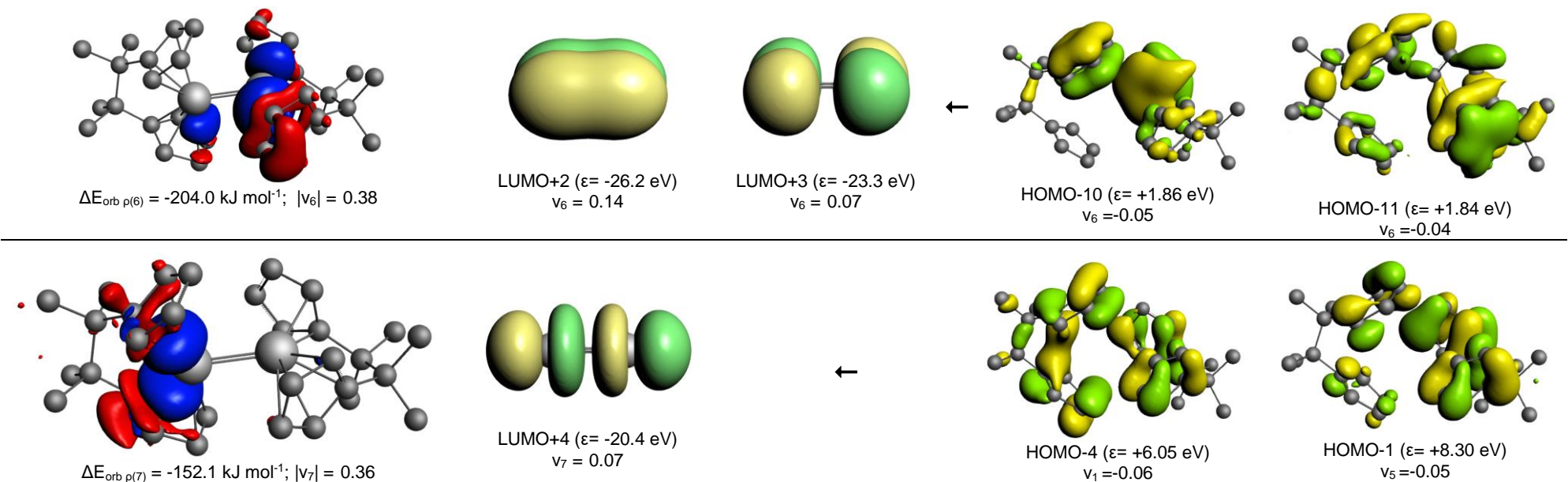


**Figure S16.** Deformation densities  $\Delta\rho$  (isovalue 0.001 a.u.) at BP86+D3(BJ)/TZ2P//M06-2X/def2-TZVPP of the pairwise orbital interactions between  $\text{Al}_2^{4+} ((\sigma_g^+)^2 (\sigma_u^+)^0)$  with  $(\text{Cp}_2(\text{CMe}_2))^2{}^{4-}$  within compound **2**. For the deformation densities the red color shows the charge outflow, whereas blue shows charge density accumulation.

---

**Cartesian xyz coordinates****2**

Energy (BP86+D3(BJ)/def2-TZVPP)= -1728.9993585 a.u.

Al	-1.160931000000	0.395631000000	0.287746000000
Al	1.204858000000	0.444070000000	-0.456306000000
C	-3.966074000000	-0.256181000000	-0.748579000000
C	-4.063916000000	-0.467951000000	0.845761000000
C	-2.803382000000	0.660451000000	-1.137193000000
C	-2.473160000000	1.973723000000	-0.580534000000
C	-1.502680000000	2.577798000000	-1.421688000000
C	-1.191442000000	1.678754000000	-2.457932000000
C	-1.979520000000	0.519323000000	-2.294998000000
C	-3.779810000000	-1.607141000000	-1.465340000000
C	-5.265133000000	0.378513000000	-1.295349000000
C	-2.679699000000	-0.609340000000	1.469616000000
C	-2.022265000000	0.348163000000	2.336176000000
C	-0.797076000000	-0.224614000000	2.793389000000
C	-0.653372000000	-1.487493000000	2.196409000000
C	-1.782241000000	-1.721387000000	1.366974000000
C	-4.814329000000	0.698587000000	1.524804000000
C	-4.870561000000	-1.740967000000	1.187337000000
C	4.206262000000	0.302080000000	0.244921000000
C	3.745117000000	-1.222624000000	0.025529000000
C	3.012997000000	1.209036000000	0.548424000000
C	2.459448000000	2.229253000000	-0.337009000000
C	1.497926000000	2.981222000000	0.404567000000
C	1.401472000000	2.425619000000	1.688641000000
C	2.311470000000	1.342092000000	1.782275000000
C	4.968040000000	0.848770000000	-0.982183000000
C	5.195525000000	0.410926000000	1.427917000000
C	2.463983000000	-1.328253000000	-0.802476000000
C	2.151926000000	-0.659987000000	-2.069153000000
C	0.951432000000	-1.231991000000	-2.585004000000
C	0.498229000000	-2.200343000000	-1.676248000000
C	1.407876000000	-2.263671000000	-0.597255000000
C	3.495219000000	-1.903560000000	1.386081000000
C	4.842443000000	-2.033340000000	-0.700255000000
H	-3.000476000000	2.477284000000	0.223636000000
H	-1.042925000000	3.546653000000	-1.248417000000
H	-0.442373000000	1.829870000000	-3.231918000000
H	-1.928150000000	-0.365260000000	-2.920227000000
H	-3.736404000000	-1.450898000000	-2.550456000000
H	-4.622582000000	-2.280060000000	-1.269262000000
H	-2.851087000000	-2.109659000000	-1.163828000000
H	-6.151020000000	-0.211182000000	-1.015235000000
H	-5.215986000000	0.415489000000	-2.392240000000
H	-5.400597000000	1.405432000000	-0.935618000000
H	-2.448551000000	1.287629000000	2.674929000000
H	-0.074623000000	0.271763000000	3.434185000000
H	0.208541000000	-2.141973000000	2.288473000000
H	-1.951128000000	-2.615966000000	0.775042000000
H	-4.385012000000	1.682180000000	1.303795000000
H	-4.796980000000	0.560884000000	2.614272000000
H	-5.864386000000	0.717172000000	1.208220000000
H	-5.026182000000	-1.789891000000	2.273935000000
H	-4.353686000000	-2.659290000000	0.887666000000
H	-5.859079000000	-1.724948000000	0.705018000000
H	2.861531000000	2.498582000000	-1.310137000000
H	0.903168000000	3.798749000000	0.008689000000
H	0.707801000000	2.736021000000	2.466325000000
H	2.451473000000	0.711272000000	2.655664000000
H	4.402262000000	0.780800000000	-1.917592000000
H	5.213453000000	1.906449000000	-0.816927000000
H	5.911312000000	0.307407000000	-1.126362000000
H	4.725994000000	0.188454000000	2.392038000000
H	5.584993000000	1.436997000000	1.479769000000
H	6.050022000000	-0.268331000000	1.292888000000
H	2.816654000000	-0.009731000000	-2.629165000000
H	0.455330000000	-0.914920000000	-3.498099000000
H	-0.428759000000	-2.763418000000	-1.754130000000
H	1.290911000000	-2.893607000000	0.278622000000
H	2.705966000000	-1.398042000000	1.959273000000
H	3.184497000000	-2.944978000000	1.233777000000
H	4.407699000000	-1.928972000000	1.993086000000
H	4.549835000000	-3.091971000000	-0.731021000000
H	4.981127000000	-1.700173000000	-1.735806000000
H	5.808132000000	-1.964735000000	-0.177323000000
X	-1.990036800000	1.482009800000	-1.578469000000
X	-1.586930600000	-0.738934200000	2.032512800000
X	1.494689200000	-1.536849000000	-1.546027200000
X	2.136662600000	2.037444400000	0.817379600000

---

**2**

Energy (M06-2X/def2-TZVPP)= -1728.2683194 a.u.

Al	1.183442000000	0.132507000000	-0.351125000000
Al	-1.244481000000	0.606321000000	-0.004510000000
C	4.038989000000	0.097905000000	0.779344000000
C	4.179591000000	-0.777042000000	-0.550174000000
C	2.848611000000	1.051690000000	0.718844000000
C	2.529081000000	1.998799000000	-0.327862000000
C	1.543828000000	2.872788000000	0.155156000000
C	1.211586000000	2.492990000000	1.458263000000
C	1.994461000000	1.386784000000	1.803458000000
C	3.882668000000	-0.800164000000	2.014047000000
C	5.304327000000	0.942290000000	1.005685000000
C	2.811172000000	-1.161336000000	-1.080705000000
C	2.173140000000	-0.635804000000	-2.238517000000
C	0.907379000000	-1.256723000000	-2.379554000000
C	0.734956000000	-2.136050000000	-1.309914000000
C	1.884351000000	-2.065574000000	-0.489226000000
C	4.955582000000	-0.027978000000	-1.645049000000
C	4.969428000000	-2.069215000000	-0.286829000000
C	-4.348387000000	0.107737000000	-0.336341000000
C	-3.785168000000	-1.138224000000	0.489793000000
C	-3.214042000000	0.879220000000	-0.983281000000
C	-2.726903000000	2.160127000000	-0.593682000000
C	-1.653451000000	2.515490000000	-1.450529000000
C	-1.455251000000	1.467369000000	-2.352000000000
C	-2.389038000000	0.449923000000	-2.057037000000
C	-5.168948000000	1.056493000000	0.553528000000
C	-5.306439000000	-0.349172000000	-1.448364000000
C	-2.474079000000	-0.819043000000	1.201430000000
C	-2.165439000000	0.346332000000	2.008593000000
C	-0.965649000000	0.096558000000	2.699647000000
C	-0.502493000000	-1.167418000000	2.338554000000
C	-1.413206000000	-1.724333000000	1.430389000000
C	-3.561124100000	-2.347962000000	-0.427589000000
C	-4.801994000000	-1.576214000000	1.558397000000
H	3.032301000000	2.100299000000	-1.274513000000
H	1.099212000000	3.676410000000	-0.410400000000
H	0.443582000000	2.935974000000	2.073929000000
H	1.939840000000	0.853434000000	2.738363000000
H	3.809661000000	-0.183800000000	2.908377000000
H	4.749065000000	-1.445673000000	2.141526000000
H	2.988562000000	-1.423151000000	1.966900000000
H	6.199645000000	0.316672000000	1.022405000000
H	5.228612000000	1.449642000000	1.967553000000
H	5.426155000000	1.704881000000	0.238812000000
H	2.600364000000	0.085705000000	-2.916015000000
H	0.188049000000	-1.046823000000	-3.154800000000
H	-0.149320000000	-2.715535000000	-1.100650000000
H	2.046111000000	-2.641201000000	0.408005000000
H	4.553647000000	0.958437000000	-1.862369000000
H	4.936598000000	-0.610774000000	-2.566094000000
H	5.997734000000	0.097596000000	-1.354611000000
H	5.149005000000	-2.578046000000	-1.234284000000
H	4.434048000000	-2.758627000000	0.362262000000
H	5.937556000000	-1.849414000000	0.166588000000
H	-3.135388000000	2.776418000000	0.190455000000
H	-1.077899000000	3.423545000000	-1.387551000000
H	-0.673194000000	1.407371000000	-3.092202000000
H	-2.480340000000	-0.485565000000	-2.585458000000
H	-4.641814000000	1.380881000000	1.447446000000
H	-5.442533000000	1.943602000000	-0.018138000000
H	-6.090486000000	0.572940000000	0.873812000000
H	-4.799152000000	-0.905770000000	-2.233268000000
H	-5.764552000000	0.527141000000	-1.907658000000
H	-6.104706000000	-0.973267000000	-1.042958000000
H	-2.808769000000	1.192326000000	2.182162000000
H	-0.474710000000	0.798535000000	3.354811000000
H	0.422182000000	-1.621560000000	2.662425000000
H	-1.306837000000	-2.691760000000	0.967297000000
H	-2.832917000000	-2.144575000000	-1.213830000000
H	-3.193127000000	-3.189090000000	0.157143000000
H	-4.492360000000	-2.667924000000	-0.890431000000
H	-4.448941000000	-2.491393000000	2.033679000000
H	-4.920544000000	-0.824641000000	2.336668000000
H	-5.780459000000	-1.779445000000	1.117002000000

## AlCp<sub>2</sub>(CMe<sub>2</sub>)<sub>2</sub>

Energy (BP86+D3(BJ)/def2-TZVPP)= -1728.99935848 a.u.

Al	-1.63414800000	0.00202100000	0.00011800000
C	1.41131300000	-0.76017600000	-0.28342800000
C	1.41321600000	0.75671700000	0.28344400000
C	0.06057400000	-1.42583600000	-0.05578800000
C	-0.56982100000	-1.72365900000	1.19804800000
C	-1.80485600000	-2.38988500000	0.94970200000
C	-1.97900700000	-2.48756600000	-0.44512800000
C	-0.85532800000	-1.87341200000	-1.07300300000
C	1.73259900000	-0.78295000000	-1.79086100000
C	2.49431900000	-1.61296900000	0.41204700000
C	0.06418800000	1.42579800000	0.05575400000
C	-0.85075700000	1.87546000000	1.07294200000
C	-1.97294700000	2.49228200000	0.44499700000
C	-1.79890700000	2.39425200000	-0.94982200000
C	-0.56540900000	1.72517700000	-1.19809100000
C	1.73447900000	0.78405100000	1.79090200000
C	2.49839800000	1.60681800000	-0.41197700000
H	-0.15672300000	-1.52015400000	2.18145200000
H	-2.51156900000	-2.71097100000	1.71041400000
H	-2.84695900000	-2.89003900000	-0.96020100000
H	-0.69211900000	-1.80094100000	-2.14389700000
H	1.67371000000	-1.82103100000	-2.15988500000
H	2.75032100000	-0.42699200000	-1.98144100000
H	1.04016800000	-0.18146700000	-2.38722400000
H	3.48827200000	-1.15138900000	0.31535000000
H	2.53600600000	-2.60354900000	-0.06204700000
H	2.28388100000	-1.76613900000	1.47681100000
H	-0.68776800000	1.80269200000	2.14384600000
H	-2.83998600000	2.89677400000	0.96002700000
H	-2.50479500000	2.71703900000	-1.71058100000
H	-0.15278200000	1.52066500000	-2.18148200000
H	1.04035200000	0.17908700000	2.38717900000
H	1.67827400000	1.81694700000	2.15991100000
H	2.75122700000	0.42009500000	1.98167400000
H	2.54251200000	2.59728900000	0.06212300000
H	2.28838900000	1.76050600000	-1.47675200000
H	3.49119700000	1.14276200000	-0.31524500000

## AlCp<sub>2</sub>(CMe<sub>2</sub>)<sub>2</sub>

Energy (M06-2X/def2-TZVPP)= -864.092817837 a.u.

Al	-1.67996500000	0.00016500000	0.00001900000
C	1.42352400000	0.75848500000	0.26237000000
C	1.42335900000	-0.75872200000	-0.26243100000
C	0.07199100000	1.41412000000	0.04041100000
C	-0.57269100000	1.65852300000	-1.20148900000
C	-1.82346800000	2.27255400000	-0.95418400000
C	-1.97960100000	2.39902300000	0.43078800000
C	-0.82842100000	1.85693300000	1.04972800000
C	1.76713600000	0.82908200000	1.75637100000
C	2.48919100000	1.59114700000	-0.46689700000
C	0.07168300000	-1.41406300000	-0.04044900000
C	-0.82875300000	-1.85686100000	-1.04974500000
C	-1.98001100000	-2.39875500000	-0.43079700000
C	-1.82391700000	-2.27217900000	0.95417000000
C	-0.57307600000	-1.65826900000	1.20146000000
C	1.76699200000	-0.82959800000	-1.75641700000
C	2.48881400000	-1.59149200000	0.46701400000
H	-0.17094200000	1.44418400000	-2.17839300000
H	-2.54374300000	2.55217700000	-1.70582500000
H	-2.84507600000	2.78634200000	0.94290500000
H	-0.65632700000	1.80414800000	2.11236600000
H	1.69463800000	1.86186800000	2.09687600000
H	2.78731600000	0.49409200000	1.93406900000
H	1.10162100000	0.22742800000	2.37354500000
H	3.47574900000	1.13211700000	-0.37591400000
H	2.53803600000	2.58405500000	-0.01895400000
H	2.26119670000	1.71683200000	-1.52368100000
H	-0.65661700000	-1.80420200000	-2.11238300000
H	-2.84552300000	-2.78599300000	-0.94291100000
H	-2.54427000000	-2.55160000000	1.70581200000
H	-0.17134100000	-1.44384600000	2.17835400000
H	1.10198800000	-0.22742700000	-2.37363900000
H	1.69336690000	-1.86233200000	-2.09690500000
H	2.78745200000	-0.49546000000	-1.93406900000
H	2.53703400000	-2.58470100000	0.01967200000
H	2.26118310000	-1.71639100000	1.52394800000
H	3.47557300000	-1.13301000000	0.37546700000

## Al<sub>2</sub>H<sub>4</sub>

Energy (BP86+D3(BJ)/def2-TZVPP)= -487.274040187 a.u.

Al	0.00000000000	0.00000000000	-1.29575500000
Al	0.00000000000	0.00000000000	1.29575500000
H	-0.96075500000	0.96110400000	-2.14577600000
H	0.96075500000	-0.96110400000	-2.14577600000
H	0.96075500000	0.96110400000	2.14577600000
H	-0.96075500000	-0.96110400000	2.14577600000

---

**Al<sub>2</sub>H<sub>4</sub>**

Energy (M06-2X/def2-TZVPP)= -487.169110261 a.u.

Al	0.000000000000	0.000000000000	-1.288089000000
Al	0.000000000000	0.000000000000	1.288089000000
H	-0.948059000000	0.949585000000	-2.124669000000
H	0.948059000000	-0.949585000000	-2.124669000000
H	0.948059000000	0.949585000000	2.124669000000
H	-0.948059000000	-0.949585000000	2.124669000000

**AlH<sub>2</sub>**

Energy (BP86+D3(BJ)/def2-TZVPP)= -243.588786815 a.u.

Al	0.000000000000	0.000000000000	0.110861000000
H	0.000000000000	1.380474000000	-0.720598000000
H	0.000000000000	-1.380474000000	-0.720598000000

**AlH<sub>2</sub>**

Energy (M06-2X/def2-TZVPP)= -243.537251659 a.u.

Al	0.000000000000	0.000000000000	0.110231000000
H	0.000000000000	1.357990000000	-0.716500000000
H	0.000000000000	-1.357990000000	-0.716500000000

**Al<sub>2</sub>Cl<sub>4</sub>**

Energy (BP86+D3(BJ)/def2-TZVPP)= -2326.25639960 a.u.

Al	0.000000000000	0.000000000000	-1.270324000000
Al	0.000000000000	0.000000000000	1.270324000000
Cl	-1.278579000000	-1.278906000000	-2.350140000000
Cl	1.278579000000	1.278906000000	-2.350140000000
Cl	-1.278579000000	1.278906000000	2.350140000000
Cl	1.278579000000	-1.278906000000	2.350140000000

**Al<sub>2</sub>Cl<sub>4</sub>**

Energy (M06-2X/def2-TZVPP)= -2325.93732022 a.u.

Al	0.000000000000	0.000000000000	-1.266219000000
Al	0.000000000000	0.000000000000	1.266219000000
Cl	-1.261594000000	1.261988000000	-2.348815000000
Cl	1.261594000000	-1.261988000000	-2.348815000000
Cl	1.261594000000	1.261988000000	2.348815000000
Cl	-1.261594000000	-1.261988000000	2.348815000000

**AlCl<sub>2</sub>**

Energy (BP86+D3(BJ)/def2-TZVPP)= -1163.07916583 a.u.

Al	0.000000000000	0.000000000000	0.776605000000
Cl	0.000000000000	1.830158000000	-0.296937000000
Cl	0.000000000000	-1.830158000000	-0.296937000000

**AlCl<sub>2</sub>**

Energy (M06-2X/def2-TZVPP)= -1162.92185122 a.u.

Al	0.000000000000	0.000000000000	0.777165000000
Cl	0.000000000000	1.806390000000	-0.297151000000
Cl	0.000000000000	-1.806390000000	-0.297151000000

---

## References

- [1] P. J. Shapiro, S.-J. Lee, P. Perrotin, T. Cantrell, A. Blumenfeld, B. Twamley, *Polyhedron* **2005**, *24*, 1366-1366.
- [2] a) R. Peloso, I. Resa, A. Rodríguez, E. Carmona, K. Freitag, C. Jones, A. Stasch, A. J. Boutland, F. Lips, P. P. Power (Ed.), *Inorg. Synth.* **2019**, Volume 37, Chapter Three; b) J. Hicks, M. Juckel, A. Paparo, D. Dange, C. Jones, *Organometallics* **2018**, *24*, 4810-4813.
- [3] G. Sheldrick, *Acta Cryst. A* **2008**, *64*, 112-122.
- [4] Y. Zhao, D. G. Truhlar, *Theor. Chem. Acc.* **2008**, *120*, 215-241.
- [5] a) A. D. Becke, *Phys. Rev. A* **1988**, *38*, 3098-3100; b) J. P. Perdew, *Phys. Rev. B* **1986**, *33*, 8822-8824.
- [6] M. J. Frisch, G. W. Trucks, H. B. Schlegel, G. E. Scuseria, M. A. Robb, J. R. Cheeseman, G. Scalmani, V. Barone, B. Mennucci, G. A. Petersson, H. Nakatsuji, M. Caricato, X. Li, H. P. Hratchian, A. F. Izmaylov, J. Bloino, G. Zheng, J. L. Sonnenberg, M. Hada, M. Ehara, K. Toyota, R. Fukuda, J. Hasegawa, M. Ishida, T. Nakajima, Y. Honda, O. Kitao, H. Nakai, T. Vreven, J. J. A. Montgomery, J. E. Peralta, F. Ogliaro, M. Bearpark, J. J. Heyd, E. Brothers, K. N. Kudin, V. N. Staroverov, R. Kobayashi, J. Normand, K. Raghavachari, A. Rendell, J. C. Burant, S. S. Iyengar, J. Tomasi, M. Cossi, N. Rega, J. M. Millam, M. Klene, J. E. Knox, J. B. Cross, V. Bakken, C. Adamo, J. Jaramillo, R. Gomperts, R. E. Stratmann, O. Yazyev, A. J. Austin, R. Cammi, C. Pomelli, J. W. Ochterski, R. L. Martin, K. Morokuma, V. G. Zakrzewski, G. A. Voth, P. Salvador, J. J. Dannenberg, S. Dapprich, A. D. Daniels, O. Farkas, J. B. Foresman, J. V. Ortiz, J. Cioslowski, D. J. Fox, Gaussian 16, Revision B.01. Gaussian, Inc., Wallingford CT, **2016**.
- [7] C. Y. Peng, P. Y. Ayala, H. B. Schlegel, M. J. Frisch, *J. Comput. Chem.* **1996**, *17*, 49-56.
- [8] J. W. McIver, A. Komornicki, *J. Am. Chem. Soc.* **1972**, *94*, 2625-2633.
- [9] H. J. Werner, M. Schütz, *J. Chem. Phys.* **2011**, *135*, 144116.
- [10] H.-J. Werner, P. J. Knowles, G. Knizia, F. R. Manby, M. Schütz, P. Celani, W. Györffy, D. Kats, T. Korona, R. Lindh, A. Mitrushenkov, G. Rauhut, K. R. Shamasundar, T. B. Adler, R. D. Amos, S. J. Bennie, A. Bernhardsson, A. Berning, D. L. Cooper, M. J. O. Deegan, A. J. Dobbyn, F. Eckert, E. Goll, C. Hampel, A. Hesselmann, G. Hetzter, T. Hrenar, G. Jansen, C. Köpli, S. J. R. Lee, Y. Liu, A. W. Lloyd, R. A. Mata, A. J. May, S. J. McNicholas, W. Meyer, T. F. Miller III, M. E. Mura, A. Nicklass, D. P. O'Neill, P. Palmieri, D. Peng, K. Pfüger, R. Pitzer, M. Reiher, T. Shiozaki, H. Stoll, A. J. Stone, R. Tarroni, T. Thorsteinsson, M. Wang, M. Welborn, <http://www.molpro.net>, **2019**.
- [11] a) R. Polly, H. J. Werner, F. R. Manby, P. J. Knowles, *Mol. Phys.* **2004**, *102*, 2311-2321; b) H. J. Werner, F. R. Manby, P. J. Knowles, *J. Chem. Phys.* **2003**, *118*, 8149-8160.
- [12] a) F. Weigend, *Phys. Chem. Chem. Phys.* **2002**, *4*, 4285-4291; b) F. Weigend, A. Köhn, C. Hättig, *J. Chem. Phys.* **2002**, *116*, 3175-3183.
- [13] a) J. P. Foster, F. Weinhold, *J. Am. Chem. Soc.* **1980**, *102*, 7211-7218; b) A. E. Reed, F. Weinhold, *J. Chem. Phys.* **1985**, *83*, 1736-1740.
- [14] A. E. Reed, R. B. Weinstock, F. Weinhold, *J. Chem. Phys.* **1985**, *83*, 735-746.
- [15] E. D. Glendening, J. K. Badenhoop, A. E. Reed, J. E. Carpenter, J. A. Bohmann, C. M. Morales, F. Weinhold, GENNBO 6.0 ed., Theoretical Chemistry Institute, University of Wisconsin, Madison, WI, **2012**.
- [16] a) R. F. W. Bader, Atoms in Molecules: A Quantum Theory, Clarendon, Oxford, **1990**; b) R. F. W. Bader, *Chem. Rev.* **1991**, *91*, 893-928.
- [17] T. A. Keith, T. K. Gristmill, 19.02.13 ed., Overland Park KS, USA ([aim.tkgristmill.com](http://aim.tkgristmill.com)), **2019**.
- [18] K. Morokuma, *J. Chem. Phys.* **1971**, *55*, 1236-1244.
- [19] a) T. Ziegler, A. Rauk, *Inorg. Chem.* **1979**, *18*, 1558-1565; b) T. Ziegler, A. Rauk, *Inorg. Chem.* **1979**, *18*, 1755-1759.
- [20] L. L. Zhao, M. von Hopffgarten, D. M. Andrade, G. Frenking, *WIREs Comput Mol Sci.* **2018**, *8*, e1345.
- [21] F. M. Bickelhaupt, N. M. M. Nibbering, E. M. Van Wezenbeek, E. J. Baerends, *J. Chem. Phys.* **1992**, *96*, 4864-4873.
- [22] a) S. Grimme, J. Antony, S. Ehrlich, H. Krieg, *J. Chem. Phys.* **2010**, *132*, 154104; b) S. Grimme, S. Ehrlich, L. Goerigk, *J. Comput. Chem.* **2011**, *32*, 1456-1465.
- [23] G. te Velde, F. M. Bickelhaupt, E. J. Baerends, C. Fonseca Guerra, S. J. A. van Gisbergen, J. G. Snijders, T. Ziegler, *J. Comput. Chem.* **2001**, *22*, 931-967.
- [24] J. P. Perdew, *Phys. Rev. B* **1986**, *33*, 8822-8824.
- [25] E. Van Lenthe, E. J. Baerends, *J. Comput. Chem.* **2003**, *24*, 1142-1156.
- [26] J. Krijn, E. J. Baerends, Fit-Functions in the HFS-Method; Internal Report (in Dutch) **1984**.
- [27] E. Van Lenthe, E. J. Baerends, J. G. Snijders, *J. Chem. Phys.* **1993**, *99*, 4597-4610.